The Electrical Impedance of Pulsatile Blood Flowing Through Rigid Tubes: A Theoretical Investigation

R. L. Gaw, B. H. Cornish*, and B. J. Thomas

***Abstract*—The electrical impedance of blood is used in biomedical applications such as impedance cardiography for monitoring blood flow. Impedance cardiography assumes a constant value for the conductivity of blood. However, this assumption has been shown to be invalid for the case of flowing blood since the conductivity is affected by flow induced changes in the orientation of red blood cells. A number of previous studies have modeled the conductivity of blood in constant flow. This study investigates the conductivity changes due to pulsatile flow as experienced during the cardiac cycle. This is achieved through the development of a theoretical model of the conductivity of pulsatile blood flowing through rigid tubes. Conductivity waveforms of pulsatile blood were generated by incorporating realistic physiological flow and cell orientation dynamics into previously reported steady flow conductivity models. Results show that conductivity correlates with the spatial average blood velocity and that features of the velocity waveform are reproduced in the conductivity signal. Conductivity was also shown to be dependent on the shape of the velocity profile. The modeled conductivity change is comparable with previously published experimental results for pulsatile blood flow, supporting the reliability of the model.**

***Index Terms*—Bioimpedance, mathematical model, pulsatile blood flow, red blood cell (RBC) orientation.**

I. Introduction

THE velocity-dependent changes in the conductivity of blood in steady flow have been widely reported in the literature [1]–[9]. Reference [1] reports that the conductivity change may be caused by changes in alignment of the red blood cells (RBCs) in response to changing shear forces. As the shear force increases, the cells experience a higher variation in velocity across their surface and so align in an orientation that will minimize this shearing stress. This orientation is with the minimum cross-sectional area facing the direction of the flow, i.e., with their major axis parallel to the direction of flow. The magnitude of the resulting conductivity changes are such that the effects are observed in applications such as impedance cardiography [1]–[3].

Previous theoretical and experimental studies have concentrated primarily on quantifying conductivity change for *constant* flow rates. As blood flowing through the heart is pulsatile in nature, these studies are not sufficient to accurately explain the conductivity change of blood flowing through the aorta and the variation of blood conductivity throughout the cardiac cycle remains largely unexplored. Although it has been demonstrated experimentally [10] that the conductivity does change during the cardiac cycle, currently no studies have been reported which theoretically model the conductivity of blood in pulsatile flow over the length of the cardiac cycle. It is expected that a greater understanding of the relationship between the velocity of pulsatile blood and the resulting conductivity changes will lead to more efficacious use of bioimpedance applications.

The mathematical model presented herein explains the flow dependence of the electrical conductivity of blood during pulsatile flow through rigid tubes. It shows that conductivity responds to changes in blood velocity over the theoretically modeled cardiac cycle. In addition, the model shows that the conductivity of blood is influenced by the velocity profile. These results demonstrate that with further research, bioimpedance waveforms may have potential to examine the flow related physiological events causing the conductivity change.

II. Theory and Methods

The conductivity of blood has been quantitatively modeled in [9] under the condition of steady laminar flow through rigid cylindrical tubes. This was achieved by extending the Maxwell–Fricke theory to include orientation and deformation of ellipsoidal particles induced by shear stresses. The model presented in the current study extends and advances the principles and assumptions used in [9] by incorporating pulsatile flow and orientation effects.

A. Assumptions of Current Model

The modeling presented assumed blood to be a flowing dilute suspension of ellipsoidal particles (the RBCs) in plasma. Each ellipsoid had two long axes (b) and one short axis (a), where $a < b$. The behavior of the RBCs was considered by assuming each cell to be centered in a small cubic control volume surrounded by plasma. These control volumes were then ordered in a regular circular pattern over the cross section of the tube as proposed in [9]. Flowing RBCs were assumed to remain in two defined states of orientation: random or aligned. Those RBCs with an orientation of $\pm 20^\circ$ to the direction of flow were assumed to be fully aligned with the flow.

Axial accumulation was ignored and blood was assumed to be a Newtonian fluid. Blood was assumed to flow in a pulsatile manner through long, straight, rigid tubes with parameters similar to those of the cardiac cycle. The driving pressure gradient was assumed to be a summation of simple harmonic motion components. The excitation current used was assumed to be dc (direct current). Since the RBC membrane acts as a capacitor at

Manuscript received November 23, 2006; revised May 3, 2007. *Asterisk indicates corresponding author.*

R. L. Gaw and B. J. Thomas are with the School of Physical and Chemical Sciences, Queensland University of Technology, Brisbane QLD 4001, Australia (e-mail: r.gaw@qut.edu.au; bj.thomas@qut.edu.au).

*B. H. Cornish is with the School of Physical and Chemical Sciences, Queensland University of Technology, GPO Box 2434, Brisbane QLD 4001, Australia (e-mail: b.cornish@qut.edu.au).

Digital Object Identifier 10.1109/TBME.2007.903531

dc, no current will flow through the cell, only the surrounding plasma. The conductivity of the intracellular fluid was therefore assumed not to contribute to the blood conductivity.

Further, although blood flow turbulence occurs during the cardiac cycle, it occurs for only a very small fraction of the cycle, and then settles quickly to laminar flow [11], [12]. Consequently, only laminar flow was modeled in this study.

B. Pulsatile Blood Flow Dynamics

The shear stress experienced by the RBCs, and its variation across the radius, is the most important factor in modeling the conductivity of blood flow. In the model developed in [9], only steady state blood flow was modeled. The addition of pulsatile flow dynamics in the present study thus advances the work presented in [9].

Fluid flows as a result of a pressure difference over the length of the tube. During flow through rigid, straight cylinders, every element of a Newtonian viscous fluid flows in a series of laminae parallel to the walls of the tube. Near a stationary surface, the fluid farther from the surface is flowing more rapidly than that closer to it. In a tube, this generates a velocity gradient perpendicular to the walls, which is referred to as the shear rate. In steady flow the velocity profile is parabolic across the diameter. In contrast, the presence of an oscillating pressure gradient, as in pulsatile flow, results in a profile that is much flatter in the central axial region. This is due to the large momenta of the laminae close to the central axial region of the tube which respond slowly to pressure changes. In contrast, laminae near to the wall have less momentum and respond more quickly.

To model the pulsatile flow velocity and shear rate, the form of the pressure gradient over the length of the tube was assumed to be simple harmonic motion and is written in complex form as

$$\frac{\mathrm{d}P}{\mathrm{d}z} = A\mathrm{e}^{\mathrm{i}\omega t} \tag{1}$$

where $\mathrm{d}P/\mathrm{d}z$ is the pressure gradient along the length z of the tube, A is the pressure coefficient (dyn·cm^{-2}) and ω is the angular frequency (rad·s^{-1}) of the oscillatory motion. The solution for simple harmonic motion is important because the use of a Fourier series expansion allows realistic blood flow waveforms to be expressed as a sum of a series of simple harmonic sine waves.

The equation for the motion of a viscous liquid in laminar flow is derived using the Navier Stokes theorem outlined in [11] and [12]. The velocity profile for flow in a tube of circular cross section and radius r undergoing an oscillatory pressure gradient, can be solved as a form of Bessel's equation resulting as [11], [12].

$$\mathbf{v}(\boldsymbol{r})(\mathrm{cm.s}^{-1}) = \frac{A}{\mathrm{i}\omega\rho}\cdot\left[1-\frac{J_0\left(\alpha\boldsymbol{y}\mathrm{i}^{\frac{3}{2}}\right)}{J_0\left(\alpha\mathrm{i}^{\frac{3}{2}}\right)}\right]\cdot\mathrm{e}^{\mathrm{i}\omega t}. \tag{2}$$

This equation was used to determine the velocity of the lamina of liquid at a fraction of the radius, $\boldsymbol{y} = r/R$, from the axis of the tube; where $\boldsymbol{v}(\mathbf{r})$ is the velocity profile of blood (cm·s^{-1}), r is the radial distance from the axial of the tube (cm), R is the radius of the tube (cm), ω is the angular frequency of the pressure pulse, ρ is the density of the fluid (g·cm^{-3}), t is time (s) and α is Womersley's number [11], [12], calculated using (3) where η is the viscosity of the fluid

$$\alpha = R\sqrt{\frac{\omega\rho}{\eta}}. \tag{3}$$

The corresponding spatial average velocity (vel) was calculated by first integrating over the cross section of the tube to find the volume flow and then dividing by the cross sectional area of the tube. This results in (4), [11], and [12]. The spatial average velocity is the average velocity of all laminae flowing through the cross section of the tube at any moment

$$\mathrm{vel}(\mathrm{cm}\cdot\mathrm{s}^{-1}) = \frac{A}{\mathrm{i}\omega\rho}\cdot\left[1-\frac{2J_1\left(\alpha\mathrm{i}^{\frac{3}{2}}\right)}{\alpha\mathrm{i}^{\frac{3}{2}}J_0\left(\alpha\mathrm{i}^{\frac{3}{2}}\right)}\right]\cdot e^{\mathrm{i}\omega t}. \tag{4}$$

The pulsatile velocity profile was then used in the present study to determine the shear stress profile of the blood. This was found by a differentiation of the velocity profile with respect to the radius (the shear rate, dv/dr), multiplied by the viscosity as shown as

$$\begin{aligned}\boldsymbol{\tau}(r)(\mathrm{N}\cdot\mathrm{m}^{-2}) &= \eta\frac{dv}{dr}\\ &= \frac{\eta A}{\mathrm{i}\omega\rho}\cdot\left[\frac{\alpha\mathrm{i}^{\frac{3}{2}}J_1\left(\alpha\mathbf{y}\mathbf{i}^{\frac{3}{2}}\right)}{J_0\left(\alpha\mathbf{i}^{\frac{3}{2}}\right)}\right]\cdot\mathrm{e}^{\mathrm{i}\omega t}.\end{aligned} \tag{5}$$

This equation encompasses the dynamics of time-varying flow and was used to determine both the RBC orientation and deformation at a location r along the radius of the tube.

C. Orientation of RBC

Reference [9] uses a simple linear relationship to determine the orientation rate of cells based on the shear rate. However, the characteristics of the cell orientation process are difficult to account for. Literature suggests that, at low shear rates, the RBCs behave as rigid disks, rotating with a periodically varying angular velocity and effectively no deformation. At higher shear rates, the cells behave more like liquid drops undergoing deformation and "tank treading" motion while achieving a stable orientation with respect to the flow [13]–[15]. Tank treading is the motion of an ellipsoid in which the cell membrane rotates around the interior cell fluid.

The transition between the two states and the degree of alignment with the flow is influenced by the shear rate profile across the tube. In the present study, it was assumed that there are only two well-defined states of orientation, this was also assumed in work reported in [2]. The states are: RBCs with random orientation, as in flipping rigid disk behavior, and RBCs in stable orientation, as in liquid drop behavior. Reference [14] assumed that all RBCs in the second state aligned with their major axis within 20° of the flow direction. To simplify the calculations, RBCs in this state were assumed parallel to the direction of flow in [9]. The present study also assumes this.

For time-varying flow, it has been reported that the times taken by RBCs to align with the flow and the time taken to disorientate also differ largely [2], [16]. This can be described as a

first-order kinetic process which is dependent on the shear rate experienced by the cells. Stop-flow experiments are described in the literature, in which blood was made to flow at a constant rate before flow was instantaneously ceased and impedance or orientation parameters were observed [2], [16]. These studies demonstrate that during accelerating flow, the impedance change (or orientation response) is essentially synchronous with the change in flow. Conversely, during deceleration of flow; exponential decay in orientation occurs with a time constant ranging in the order of 1 to 100 s.

Equation (6) shows an approximate expression for the orientation rate as a function of shear rate across the radius of the tube presented in [14]:

$$\boldsymbol{f}(r) = \frac{n}{n_0} = \frac{\boldsymbol{\tau}_{\mathrm{o}}^{-1}(r)}{\boldsymbol{\tau}_{\mathrm{d}}^{-1}(r) + \boldsymbol{\tau}_{\mathrm{o}}^{-1}(r)} \tag{6}$$

where n is the number of RBCs with stable orientation per unit volume (in this case, assumed to be oriented parallel to the flow), n_0 is the total number of RBCs per unit volume, τ_{o} is the time constant for cells changing from random to aligned orientation and τ_{d} is the time constant for cells changing from aligned to random orientation. Bitbol and Quemada [14] proposed that the time constant for cell orientation (τ_{o}) is proportional to the inverse of the shear rate and the time constant for cell disorientation (τ_{d}) is proportional to the inverse of the square root of the shear rate.

D. Deformation of RBC

For the present study, the calculation of RBC deformation presented by in [9] was used. When blood flows, RBCs deform due to the velocity gradient of laminae (shear stress) across the radius. Since the shear stress is radially dependent, the amount of deformation is also dependent on r and is indicated by a change in the ratio of the short to long axes of the cell. The relationship between the cell axis ratio $(a_{\mathrm{d}}/b_{\mathrm{d}})$ after deformation, and shear stress developed in [9] is shown as follows:

$$\frac{\boldsymbol{a}_{\mathrm{d}}(r)}{\boldsymbol{b}_{\mathrm{d}}(r)} = \frac{a_0}{b_0}\left[1 + \frac{\boldsymbol{\tau}(r) b_0}{4\mu}\right]. \tag{7}$$

An RBC with initial axis lengths of a_0 and b_0 is deformed in the presence of a shearing stress $\boldsymbol{\tau}(r)$ at a distance r from the tube axis. The new axial lengths are a_{d} and b_{d}, respectively, and μ is the surface shear modulus of the cell membrane.

E. Conductivity of Blood

The conductivity of a representative control volume was calculated using the highly cited Maxwell–Fricke equations as illustrated in [9]. For a single control volume located at a distance r from the axis, the conductivity was calculated using the following:

$$\frac{\sigma_{\mathrm{cv}}}{\sigma_{\mathrm{pl}}} = \frac{1-h}{1+(C-1)\cdot h} \tag{8}$$

where σ_{cv} and σ_{pl} are the conductivities $(\mathrm{S{\cdot}m^{-1}})$ of the control volume and the plasma, respectively, h is the haematocrit expressed as a fraction, and C is a factor that depends on the geometry and orientation of the RBC at location r.

For a control volume in which the contained cell is oriented with its short axis (a) or long axis (b) parallel to the electric field, and also the flow direction, C is calculated as follows:

$$C_a = \frac{1}{M}, \quad C_b = \frac{2}{2-M} \tag{9}$$

$$M(a<b) = \frac{\varphi - \frac{1}{2}\sin(2\varphi)}{\sin^3(\varphi)} \cdot \cos(\varphi), \cos(\varphi) = \frac{a}{b}. \tag{10}$$

For cells in random orientation, it is assumed that cells are equally distributed in orientation between the three axes aligned with the flow. C is calculated by taking the average of the C values for each axis alignment as shown follows:

$$C_r = \frac{1}{3}(C_a + 2C_b). \tag{11}$$

The deformation of a RBC experiencing different shear stresses is accounted for by using the deformed short to long axis ratio in calculating M of (10). The C factor in the calculation of the control volume conductivity using Maxwell–Fricke equations must encompass the orientation state of the cells. To incorporate the orientation effect, C does not require the precise orientation to be known. It relies on the fraction of aligned cells, $\mathbf{f}(r)$ and the fraction of randomly oriented cells. The calculation of C based on the fraction of aligned cells is introduced in this study as follows:

$$\boldsymbol{C}(r) = \boldsymbol{f}(r)\cdot C_b + (1 - \boldsymbol{f}(r))\cdot C_r. \tag{12}$$

The bulk conductivity of blood shown in (13) is calculated by a summation of the control volume conductivities over the cross section and Ohm's Law as proposed in [9]:

$$\sigma_{\mathrm{bl}}(\mathrm{S\cdot m^{-1}}) = \frac{2}{R^2}\int_0^R \boldsymbol{\sigma}_{\mathrm{cv}}(r) r \mathrm{d}r. \tag{13}$$

The conductivity of stationary blood was also calculated [see (8)] where $C = C_r$. This allowed the change in conductivity of flowing blood from the constant conductivity of stationary blood used in impedance cardiography to be calculated as follows:

$$\Delta\sigma(\%) = \left(\frac{\sigma_{\mathrm{bl}} - \sigma_{\mathrm{st}}}{\sigma_{\mathrm{st}}}\right) \times 100. \tag{14}$$

III. Results

Results published in [9] have been recreated in Fig. 1(a) using the previously published method and parameters. Fig. 1(a) shows the change in conductivity from stationary blood as a function of reduced average velocity. The reduced average velocity is defined as the ratio of the average velocity to the tube radius $(\langle \mathrm{v} \rangle / R)$. Comparison of Fig. 1 and [9, Fig. 5(a)] shows good agreement.

Fig. 1(b) shows the application of the steady flow model published in [9] to a pulsatile velocity waveform flowing through a rigid tube of 10 mm at 72 beats per minute (bpm) for a haematocrit of 45%. This result is important because it demonstrates that steady-state models fail when applied to pulsatile blood flow. This is because acceleration is an important factor in determining the conductivity of flowing blood. Experimental results published in [6] show that for the same average velocity,

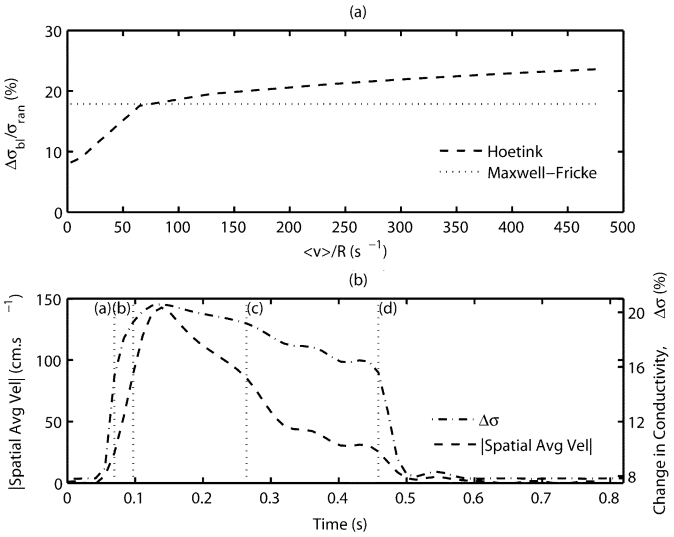

Fig. 1. Results of steady flow methods. (a) Conductivity change of blood as a function of reduced average velocity as modeled in [16, Fig. 5(a)]. (b) Modeled conductivity change from pulsatile average velocity based on steady flow calculations in [16] over one cardiac cycle, h $= 45\%, R = 5$ mm, pulse rate $= 72$ bpm (a) t $= 0.07$ s, (b) t $= 0.10$s, (c) t $= 0.26$ s, (d) t $= 0.46$ s.

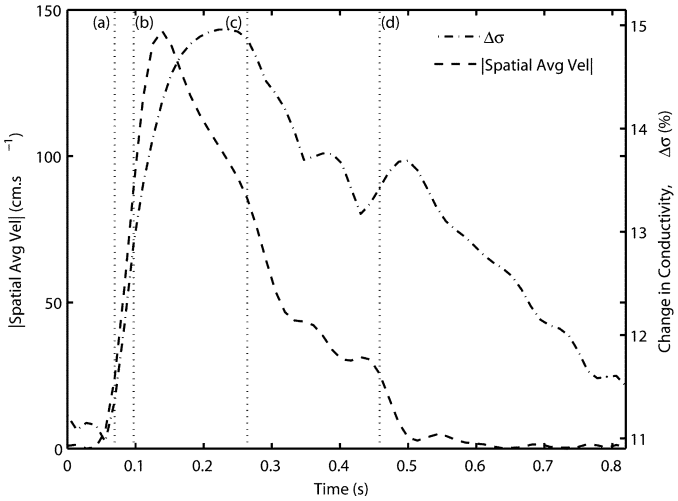

Fig. 2. Modeled absolute spatial average velocity and conductivity change from stationary blood over one cardiac cycle, h $= 45\%, R = 5$ mm, pulse rate $= 72$ bpm, (a) t $= 0.07$ s, (b) t $= 0.10$ s, (c) t $= 0.26$ s, (d) t $= 0.46$ s.

TABLE I
MODELING PARAMETERS

Parameter	Description	Value
h	Haematocrit of blood	0.45
ρ	Density of blood	1.055 g.ml^{-1}
η_{bl}	Viscosity of blood	η_{pl}(1+2.5h+0.0732h) Poise
η_{pl}	Viscosity of plasma	0.0135 Poise
μ	Membrane shear modulus of cell	0.000015 N.m^{-1}
$2b_0$	Major axis length of RBC	8 μm
N	Number of harmonics	10
f	Frequency of heartbeat	1.2 Hz (72 bpm)
R	Radius of tube	5 mm

the conductivity of flowing blood is different for accelerating and decelerating flow. In Fig. 1(b), the vertical lines labeled (a) to (d) identify times at which the average velocity is the same [times (a) and (d) and times (b) and (c)] under acceleration and deceleration. The corresponding conductivity is the same at both times. Due to inherent differences in the shear profile of steady and pulsatile flow, the steady-state model is shown to fail when applied to pulsatile blood flow.

To model the conductivity in this study, realistic flow parameters were selected (see Table I). The flow waveform displayed a peak velocity of approximately 140 cm·s^{-1} and a normal resting pulse rate of 72 bpm, typical of a healthy adult. This flow was derived from the pressure gradient across the aorta and is shown for one cardiac cycle by the dashed line in Fig. 2. The vertical lines labeled (a) to (d) are for the same velocities indicated in Fig. 1(b).

The derived velocity profile and shear stress profile at different times during the flow [as indicated by the vertical lines in Fig. 2 labeled (a) to (d)] are shown in Fig. 3. It can be seen that the velocity profiles are not parabolic as in the case of steady flow, but display characteristics of pulsatile flow such as flattening of the central velocity profile and high shear rates closer to the wall of the tube. It should also be noted that the velocity and shear stress profiles are not the same at time (a) and (d), and time (b) and (c), despite the fact that they represent the same spatial average velocity.

The result for the change in conductivity of pulsatile human blood as a percentage from stationary blood over one cardiac cycle is also shown in Fig. 2 by the dot-dashed line with the corresponding absolute spatial average velocity. The acceleration phase of the cycle for the absolute spatial average velocity occurs from 0 to 0.14 s and the deceleration phase for the spatial average velocity from 0.14 s to the end of the cycle.

The absolute spatial average velocity is used for comparisons to conductivity curves because conductivity is a nondirectional parameter. That is, the bulk conductivity and therefore the percentage change in conductivity of blood is dependent on the magnitude of shear contributing to the orientation of the flowing cells rather than the positive or negative direction of the flow. The use of the absolute spatial average velocity is easier for identification of orientation changes caused by velocity and acceleration changes.

The modeled results show that changes in the absolute spatial average velocity affect the percentage conductivity change from stationary blood. For the acceleration phase of the data presented, a strong linear relationship between the absolute spatial average velocity and the bulk conductivity of blood is seen $(r^2 = 0.99)$. This demonstrates that the changes in conductivity follow closely the changes in spatial average velocity. However, during the deceleration phase, a delay is evident in the conductivity response to changes in absolute spatial average velocity. In addition, the percentage conductivity change, and therefore the bulk conductivity, is also different between acceleration and

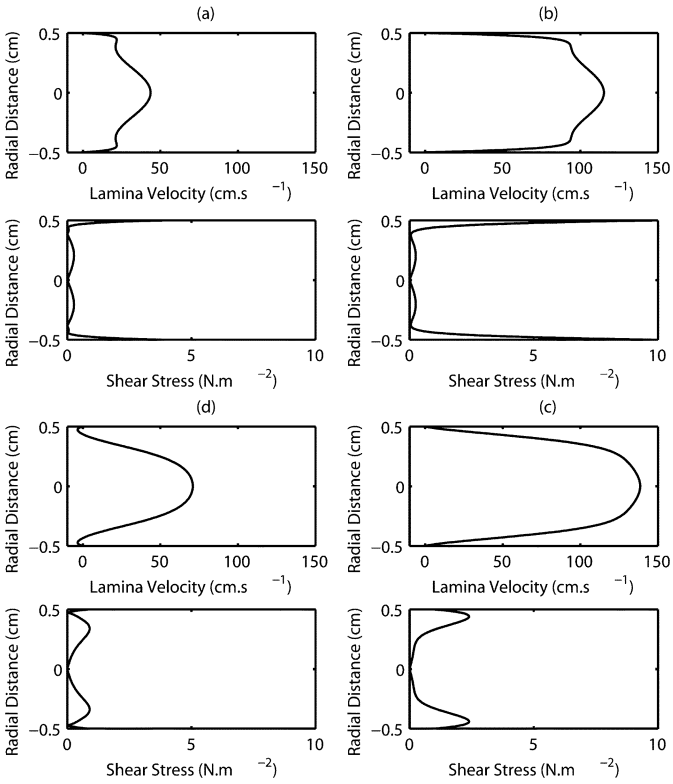

Fig. 3. Velocity and shear stress profiles at different times during pulsatile flow, (a) $t = 0.07$ s, (b) $t = 0.10$ s, (c) $t = 0.26$ s, (d) $t = 0.46$ s.

deceleration of blood at the same velocity, for example, at times (a) and (d), and (b) and (c) in Fig. 2.

IV. Discussion

The features of velocity seen during the deceleration phase between 0.3 and 0.5 s (see Fig. 2) are clearly repeated, although delayed, in the conductivity change waveform. This suggests that there exist some nonlinear characteristics throughout the modeled cycle. The relationship between the velocity and conductivity over time is shown explicitly in Fig. 4. This figure shows the absolute average spatial velocity and the corresponding conductivity at each time during the cycle. The spatial average acceleration of the blood is also indicated by the color map.

Published stop-flow experiments in [2] report that the conductivity responds instantaneously to increases in velocity. Fig. 4 confirms this as the conductivity is linear with velocity during acceleration. Additionally, it is reported in [2] that the conductivity response decays when the flow is stopped suggesting that the cells take time to disorientate. This effect can be seen in the modeling results presented in Figs. 2 and 4 between 0.5 s and the end of the cycle when the absolute spatial average velocity has returned to approximately zero. Throughout this time, the conductivity change is still decreasing, confirming the decay effect reported in the literature. Between 0.14 and 0.5 s of the deceleration phase, the decay effect is less noticeable but still clearly exists. During this time, the blood remains in motion and cells are not able to disorientate freely due to the shear stresses involved.

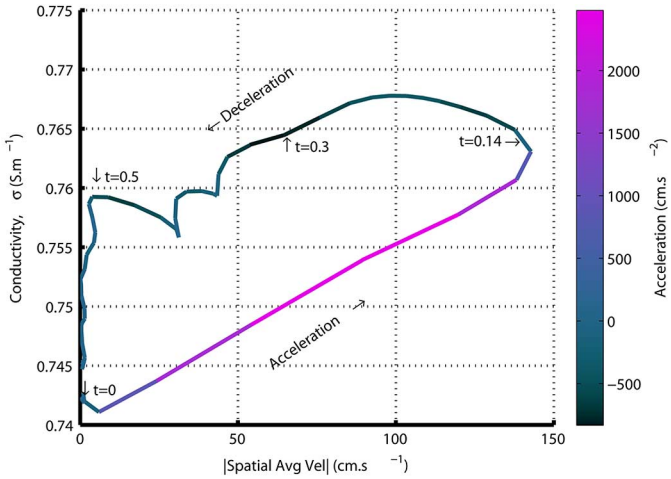

Fig. 4. Conductivity versus absolute spatial average velocity with acceleration indicated by color variations.

The important aspect to note from this is that the relationship between the absolute spatial average velocity and the conductivity changes during the cardiac cycle. This relationship changes as the spatial average velocity begins to change from accelerating to decelerating. As the blood decelerates, the relationship is no longer the same as that for acceleration and becomes less linear at lower velocities. Fig. 4 also shows explicitly that the conductivity during pulsatile flow is not the same, at any given velocity during acceleration and deceleration. This is suggested to be due to differences in the shape of the velocity profile of the blood during these times. In Figs. 2 and 3 the velocity and particularly the shear stress profiles at times (a) and (d), and (b) and (c), are significantly different. This is despite the fact that the spatial average velocity is the same for each pair of times. At each instant, the cells are changing orientation in response to individual lamina velocities resulting in differences in conductivity. This again emphasizes the importance of the velocity profile in determining the conductivity of blood.

Fig. 2 also shows a time delay in the response of conductivity during the deceleration phase. During oscillatory flow of viscous fluids, it has been previously mentioned that the central axial region of the velocity profile is largely flattened. The central axial laminae act like a solid core with high momentum and therefore resist changes in pressure. Hence, the velocity response of the central axial laminae is delayed from that of the bulk spatial average velocity. Conversely, the velocity response of the laminae closer to the walls precedes changes in the spatial average velocity. This would suggest that it is the flattened central core of the flowing blood which has the greatest effect on conductivity. To investigate this, the cross correlation between two time series was calculated, and the value for zero delay recorded. This was completed for each individual radial lamina velocity waveform and the observed bulk conductivity waveform. These data are presented in Fig. 5, together with the correlation of the absolute spatial average velocity and bulk conductivity. The higher correlation for laminae with radial fractions less than 0.6 to 0.7 support this proposal that the central core of the flowing blood is primarily responsible for the bulk conductivity. Varying the parameters of haematocrit, cell size

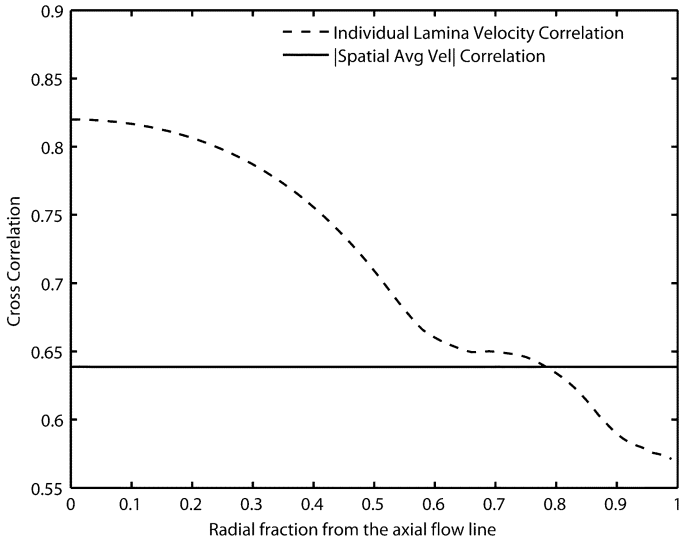

Fig. 5. Correlation between conductivity and lamina velocity at a fraction of the radius.

and pulse rate show no significant change in the radial fraction of laminae contributing to the bulk conductivity. Decreasing the radius by 50% also shows no significant fraction change. When the radius is increased by up to 250%, a second peak of laminae cross correlation is found at a radial fraction between 0.7 and 0.9.

The conductivity dependence on the central axial laminae also explains why there is only a small peak-to-peak conductivity change over the duration of the pulse of approximately 4% in Fig. 2. The flattening effect of the solid core existing in pulsatile flow results in a small variation in velocity across the inner radial laminae. The cells in this region will therefore experience small shear effects and thus the orientation of these cells will be altered only minimally during flow. The consequence of this is a smaller change in conductivity over the duration of the pulse. Peak-to-peak changes of similar magnitudes have also been reported in [6] for pulsatile flow.

Despite this small peak-to-peak percentage change modeled, literature suggests that blood flow-related conductivity changes are indeed observed in applications such at impedance cardiography [1]–[3]. These impedance changes may be as small as 1 Ω; however, they remain significant, as it is the patterns found within the waveform that may prove useful in interpreting physiological causes [17].

There exists limited literature presenting experimental results for pulsatile blood flow. The experimental results reported in [6, Fig. 1] are for the longitudinal conductance (G_{x3}) of pulsatile blood flowing through a rectangular tube. Despite the difference in experimental setup, similar characteristics are shared with the modeled results such as instantaneous conductivity response during acceleration and decaying conductance during deceleration. The theoretical results presented in Fig. 4 of the present study also match the general shape of the experimental results reported in [6, Fig. 7]. In particular, the linear relationship between average velocity and conductivity during acceleration, and the decay observed in conductivity during deceleration are evident in both the theoretical model presented here and the experimental results of [6].

Without further published results for comparison to pulsatile flow, previously published steady state results (both theoretical and experimental) [2]–[4], [6], [8], [9] were used for comparison to the theoretical model presented here. First, comparison of the theoretical conductivity results in Fig. 1(b) (calculated using steady-state methods defined in [9]) and Fig. 2 (calculated using pulsatile flow methods outlined in the present study) for the same spatial average velocity waveform, show that the inclusion of pulsatile flow significantly effects, not only the shape of the conductivity waveform, but also the magnitude of the change (e.g., by a factor of almost a half at times surrounding the peak velocity).

The theoretical results of the present study were also compared to previously published steady flow results. This was achieved by modifying the parameters of the present theoretical model to match those of the previously published experimental configurations. In each case, the theoretically calculated conductivity change at the peak spatial average velocity for pulsatile blood flow was used as a steady-state flow comparison. The results show that the theoretical conductivity change is less than that predicted for the same steady flow rates. For example, modeling results presented in [9] demonstrate a 25% change in conductivity at a reduced average velocity of 500 s^{-1}, tube diameter of 4 mm, and haematocrit of 47.5%. The theoretical model in the present study calculates a conductivity change of only 18% for these parameters.

These differences are because of the characteristics of pulsatile flow and the dependence of the conductivity on the inner axial region. As previously identified, the velocity of the central axial region is delayed from the spatial average velocity. As blood begins to flow, the RBCs do not have time to fully align with the flow before the flow changes direction. As the flow direction changes more often, such as in the case of increased heart rate, the orientation of the RBC is not able to follow the rapid changes in flow. This means that the conductivity does not reach the same as that predicted in steady flow and demonstrates that steady flow models are not accurate in determining the conductivity of pulsatile blood flow. This effect was also observed experimentally in [5] for blood flowing through rectangular tubes.

V. Conclusion

It has been theoretically shown that evidence of RBC orientation changes are present within conductivity waveforms of pulsatile blood flowing through rigid tubes. This implies that information indicative of the velocity and velocity profile of the blood may be obtained from the conductivity waveform. Further development of this model to include more complex flow dynamics through tubes with flexible walls may prove useful in *in-vivo* blood flow applications such as impedance cardiography.

References

[1] K. R. Visser, R. Lamberts, and W. G. Zijlstra, "Origin of the impedance cardiogram," in *Proc. 10th Annu. Int. Conf. IEEE Eng. Med. Biol. Soc.*, 1988, vol. 2, pp. 763–765.

[2] K. R. Visser, "Electric properties of flowing blood and impedance cardiography," *Ann. Biomed. Eng.*, vol. 17, pp. 463–473, 1989.
[3] P. M. de Vries, J. W. Langendijk, and P. M. Kouw, "The influence of alternating current frequency on flow related admittance changes of blood: A concept for improvement of impedance cardiography," *Physiol. Meas.*, vol. 16, pp. 63–69, 1995.
[4] F. M. Liebman, J. Pearl, and S. Bagno, "The electrical conductance properties of blood in motion," *Phys. Med. Biol.*, vol. 7, pp. 177–194, 1962.
[5] F. M. Liebman and S. Bagno, "The behavior of red blood cells in flowing blood which accounts for conductivity changes," *Biomed. Sci. Instrum.*, vol. 4, pp. 25–35, 1968.
[6] J. W. Dellimore and R. G. Gosling, "Change in blood conductivity with flow rate," *Med. Biol. Eng.*, vol. 13, pp. 904–913, 1975.
[7] K. Sakamoto and H. Kanai, "Electrical characteristics of flowing blood," *IEEE Trans. Biomed. Eng.*, vol. BE-26, no. 12, pp. 686–695, Dec. 1979.
[8] K. R. Visser, "Electric conductivity of stationary and flowing human blood at low frequencies," *Med. Biol. Eng. Comput.*, vol. 30, pp. 636–640, 1992.
[9] A. E. Hoetink, T. J. C. Faes, K. R. Visser, and R. M. Heethaar, "On the flow dependency of the electrical conductivity of blood," *IEEE Trans. Biomed. Eng.*, vol. 51, pp. 1251–1261, 2004.
[10] E. Raaijmakers, J. T. Marcus, H. G. Goovaerts, P. M. J. M. de Vries, Th. J. C. Faes, and R. M. Heethaar, "The influence of pulsatile flow on blood resistivity in impedance cardiography," in *Proc. 18th Annu. Int. Conf. IEEE Eng. Med. Biol. Soc.*, 1996, pp. 1957–1958.
[11] D. A. McDonald, *Blood Flow in Arteries.*. London, U.K.: Edward Arnold, 1974, pp. 17–173.
[12] M. Zamir, *The Physics of Pulsatile Flow*. New York: Springer-Verlag, 2000, pp. 1–112.
[13] S. R. Keller and R. Skalak, "Motion of a tank treading ellipsoidal particle in shear flow," *J. Fluid Mech.*, vol. 120, pp. 27–47, 1982.
[14] M. Bitbol and D. Quemada, "Measurement of erythrocyte orientation in flow by spin labeling II—Phenomenological models for erythrocyte orientation rate," *Biorheology*, vol. 22, pp. 31–42, 1985.
[15] M. Bitbol, "Red blood cell orientation in orbit $C = 0$," *Biophys. J.*, vol. 49, pp. 1055–1068, 1986.
[16] M. Bitbol and F. Leterrier, "Measurement of erythrocyte orientation in a flow by spin labeling," *Biorheology*, vol. 19, pp. 669–680, 1982.
[17] R. A. Peura, B. C. Penney, J. Arcuri, F. A. Anderson, Jr., and H. B. Wheeler, "Influence of erythrocyte velocity on impedance plethysmographic measurements," *Med. Biol. Eng. Comput.*, vol. 16, pp. 147–154, 1978.

R. L. Gaw, photograph and biography not provided at the time of publication.

B. H. Cornish, photograph and biography not provided at the time of publication.

B. J. Thomas, photograph and biography not provided at the time of publication.